Very oblique whistler generation by low-energy electron streams

Didier Mourenas, A. V. Artemyev, O. V. Agapitov, V Krasnoselskikh, F.S. Mozer

AGU PUBLICATIONS

JGR

Journal of Geophysical Research: Space Physics

RESEARCH ARTICLE

10.1002/2015JA021135

Very oblique whistler generation by low-energy electron streams

D. Mourenas[1], A. V. Artemyev[2], O. V. Agapitov[3,4], V. Krasnoselskikh[2], and F. S. Mozer[3]

[1]CEA, DAM, DIF, Arpajon, France, [2]LPC2E/CNRS-University of Orleans, Orléans, France, [3]Space Science Laboratory, University of California, Berkeley, California, USA, [4]Astronomy and Space Physics Department, National Taras Shevchenko University of Kiev, Kiev, Ukraine

Key Points:

- Very oblique chorus waves could be generated by low-energy beams or streams
- Landau and cyclotron resonance generation mechanisms are examined analytically
- Analytical frequency sweep rates correspond with Van Allen Probes measurements

Correspondence to:
D. Mourenas,
didier.mourenas@gmail.com

Citation:
Mourenas, D., A. V. Artemyev, O. V. Agapitov, V. Krasnoselskikh, and F. S. Mozer (2015), Very oblique whistler generation by low-energy electron streams, *J. Geophys. Res. Space Physics*, *120*, 3665–3683, doi:10.1002/2015JA021135.

Received 17 FEB 2015
Accepted 12 APR 2015
Accepted article online 22 APR 2015
Published online 25 MAY 2015

Abstract Whistler mode chorus waves are present throughout the Earth's outer radiation belt as well as at larger distances from our planet. While the generation mechanisms of parallel lower band chorus waves and oblique upper band chorus waves have been identified and checked in various instances, the statistically significant presence in recent satellite observations of very oblique lower band chorus waves near the resonance cone angle remains to be explained. Here we discuss two possible generation mechanisms for such waves. The first one is based on Landau resonance with sporadic very low energy (<4 keV) electron beams either injected from the plasma sheet or produced in situ. The second one relies on cyclotron resonance with low-energy electron streams, such that their velocity distribution possesses both a significant temperature anisotropy above 3–4 keV and a plateau or heavy tail in parallel velocities at lower energies encompassing simultaneous Landau resonance with the same waves. The corresponding frequency and wave normal angle distributions of the generated very oblique lower band chorus waves, as well as their frequency sweep rate, are evaluated analytically and compared with satellite observations, showing a reasonable agreement.

1. Introduction

Whistler mode waves are rather ubiquitous in the magnetosphere of the Earth, although their wave power generally increases at times of stronger geomagnetic activity [*Burtis and Helliwell*, 1969; *Tsurutani and Smith*, 1974; *Li et al.*, 2010; *Agapitov et al.*, 2013; *Orlova and Shprits*, 2014]. Bursty whistler mode waves with frequencies $\omega \sim 0.1-0.8\Omega_{ce}$ (where Ω_{ce} is the electron gyrofrequency) which appear as either rising tones, falling tones, or hooks at $L \sim 4-10$ are generally called chorus emissions. Observed from the equator up to high magnetic latitudes and mainly from 22:00 to 14:00 magnetic local time (MLT), they are among the most intense electromagnetic emissions recorded inside the magnetosphere [*Meredith et al.*, 2012; *Li et al.*, 2010, 2013a; *Agapitov et al.*, 2013].

Their source region is thought to be close to the geomagnetic equator [*LeDocq et al.*, 1998; *Santolík et al.*, 2009; *Omura et al.*, 2009] where the magnetic field inhomogeneity is minimal, but it may extend up to a few thousand kilometers along field lines as well as in the transverse direction [*Santolík et al.*, 2005; *Agapitov et al.*, 2010]. Anisotropic and warm (1–50 keV) electron populations injected from the plasma sheet during substorms are believed to provide the necessary energy for chorus wave generation via linear and nonlinear processes [e.g., see *Kennel and Petschek*, 1966; *Li et al.*, 2010; *Omura et al.*, 2008; *Cully et al.*, 2011].

Chorus waves most often occur in two distinct frequency bands: the lower band ($0.1 < \omega/\Omega_{ce} < 0.45$) and the upper band ($0.55 < \omega/\Omega_{ce} < 0.8$) [*Tsurutani and Smith*, 1974; *Hayakawa et al.*, 1984; *Meredith et al.*, 2012]. The gap near $\Omega_{ce}/2$ could result from nonlinear damping of weakly oblique waves propagating along an inhomogeneous geomagnetic field [*Omura et al.*, 2009; *Yagitani et al.*, 2014]. Upper band and lower band chorus waves could also be separately excited inside ducts of depleted and enhanced density, respectively [*Bell et al.*, 2009]. More recently, *Fu et al.* [2014] demonstrated via numerical simulations using measured electron populations with large enough temperature anisotropies that a low-energy (~300 eV) population could drive quasi-electrostatic very oblique upper band chorus waves while a hotter (> 2 keV) component was generating quasi-parallel lower band chorus waves. The gap at $\Omega_{ce}/2$ is then simply the consequence of the linear excitation of two distinct whistler modes by two well-separated electron populations. Nonetheless, individual chorus elements crossing this gap have sometimes been reported too [*Burtis and Helliwell*, 1976; *Kurita et al.*, 2012].

Chorus waves have been shown to play a prominent role in the dynamics of trapped electrons at $L \sim 4$–8, being often responsible for the main losses and accelerations of energetic ($E \sim 5$ keV to 5 MeV) electrons [*Horne et al.*, 2005; *Thorne et al.*, 2010; *Li et al.*, 2013b; *Thorne et al.*, 2013; *Chen et al.*, 2014], although other kinds of waves and other processes can also be important [*Thorne*, 2010; *Mozer et al.*, 2013, 2014].

Quasi-linear and nonlinear models of wave-particle interaction generally assume that chorus waves propagate at wave normal angles nearly parallel to geomagnetic field lines [e.g., see *Nunn*, 1971; *Karpman et al.*, 1974; *Albert*, 2002; *Trakhtengerts et al.*, 2004; *Omura et al.*, 2008; *Nunn et al.*, 2009; *Orlova and Shprits*, 2014], although some studies have also considered very oblique waves [*Bell*, 1984; *Inan and Bell*, 1991; *Shklyar and Matsumoto*, 2009; *Mourenas et al.*, 2012a, 2012b; *Artemyev et al.*, 2012].

The latest studies considering electron interactions with very oblique waves have been motivated by recent satellite statistics showing high occurrences of very oblique lower band chorus waves, especially during quiet or moderately disturbed geomagnetic conditions [*Li et al.*, 2013a; *Agapitov et al.*, 2013; *Artemyev et al.*, 2013a; *Mourenas et al.*, 2014] and even near the equator [*Santolík et al.*, 2009; *Li et al.*, 2013a; *Mourenas et al.*, 2014; *Taubenschuss et al.*, 2014], although quasi-parallel waves are generally prevalent at magnetic latitudes lower than ∼35° [*Hayakawa et al.*, 1984]. These results have been globally confirmed by ray tracing simulations of lower band chorus wave propagation to higher latitudes after their generation near the equator [*Chen et al.*, 2013].

Following the classification adopted in these previous studies, one can distinguish quasi-parallel or moderately oblique whistlers, with a wave normal angle within 30°–45° of the background magnetic field direction, from very oblique whistlers with higher wave normal angles close to the resonance cone angle. An analysis of conjunction events between Polar Operational Environmental Satellites and the Van Allen Probes has recently suggested that such very oblique lower band chorus waves could play a significant role in scattering 30–100 keV electrons into the loss cone during moderately disturbed periods [*Li et al.*, 2014]. High-amplitude very oblique waves have also been observed [*Cattell et al.*, 2008; *Cully et al.*, 2008; *Agapitov et al.*, 2014], stimulating the development of nonlinear models describing the trapping, acceleration, and also the possible bursty losses of 10–100 keV electrons induced by these waves [*Artemyev et al.*, 2012, 2013b, 2014a; *Osmane and Hamza*, 2014]. However, the exact generation mechanism of such very oblique whistler mode waves near the equator still remains something of a mystery.

In the present paper, we first provide in section 2 useful analytical estimates of the energy of electrons potentially interacting via Landau or cyclotron resonance with lower band chorus waves. In the next section, we make use of various satellite observations of low-energy electrons and lower band chorus waves to discuss the most probable generation mechanisms of these waves. Section 4 is then devoted to approximate analytical calculations of the corresponding frequency sweep rates of very oblique lower band chorus waves, allowing finally some comparisons with frequency sweep rates observed by satellites.

2. Interaction of Low-Energy Electrons With Oblique Lower Band Chorus Waves

2.1. Generalities

The oblique whistler mode wave dispersion relation in a cold magnetized plasma reads as [e.g., see *Lyons*, 1974; *Verkhoglyadova et al.*, 2010]

$$\mu^2 = \frac{k^2c^2}{\omega^2} = 1 + \frac{\Omega_{pe}^2}{\omega(\Omega_{ce}\cos\theta - \omega)} \tag{1}$$

with μ is the refractive index, k the wave number, θ the wave normal angle between the wave vector and the background magnetic field, c the velocity of light and where we consider only oblique whistler mode waves with frequency ω much higher than the Lower Hybrid frequency and smaller than half the electron gyrofrequency $\sqrt{\Omega_{ce}\Omega_{ci}} \ll \omega < \Omega_{ce}/2$ in situations such that $\Omega_{pe}^2 \gg \Omega_{ce}^2$. Here Ω_{ci}, Ω_{ce}, and Ω_{pe} are the local ion gyrofrequency, electron gyrofrequency, and plasma frequency, respectively.

The wave group velocity $V_g = \partial\omega/\partial k$ along the wave vector direction is given by

$$V_g = \frac{2c\cos\theta\Omega_{ce}}{\Omega_{pe}} \frac{(\Omega_{ce}\cos\theta - \omega)^{3/2}\omega^{1/2}}{\Omega_{ce}^2\cos^2\theta} \tag{2}$$

leading to a parallel group velocity $V_{g\parallel} = \partial\omega/\partial k_\parallel \sim V_g k/k_\parallel$ along the geomagnetic field line

$$V_{g\parallel} \simeq \frac{2c\Omega_{ce}}{\Omega_{pe}} \frac{(\Omega_{ce}\cos\theta - \omega)^{3/2}\omega^{1/2}}{\Omega_{ce}^2 \cos^2\theta} \tag{3}$$

while the parallel phase velocity $V_{P\parallel} = \omega/k_\parallel$ is

$$V_{P\parallel} \simeq \frac{c\sqrt{\omega(\Omega_{ce}\cos\theta - \omega)}}{\Omega_{pe}\cos\theta}. \tag{4}$$

From the above expressions, the highest parallel phase velocity is reached for $\theta = \theta_g$ with θ_g the Gendrin angle defined by $\cos\theta_g = 2\omega/\Omega_{ce}$. At still higher θ, both the parallel group and phase velocities decrease.

2.2. Wave-Particle Interactions Via Landau Resonance

When addressing wave-particle resonant interactions, two main resonances must be considered in general: the Cerenkov-Landau resonance and the first-order cyclotron resonance [*Shklyar and Matsumoto*, 2009]. Landau resonance corresponds to a resonant electron parallel velocity $V_{R\parallel}$ such that

$$V_{R\parallel} = V_{P\parallel}. \tag{5}$$

Landau resonance occurs during the bounce motion of electrons from the equator to their mirror point [*Lyons et al.*, 1972]. Considering particles with a fixed pitch angle, it follows immediately from equations (4) and (5) that the energy of resonant electrons is always minimal for waves such that $\theta \geq \theta_g$. However, there exists also an upper bound on θ for whistler mode waves in a cold plasma, corresponding to the so-called resonance cone angle θ_r. For $\omega^2 \ll \Omega_{pe}^2$, one gets $\cos\theta_r \simeq \omega/\Omega_{ce}$. At the resonance cone angle, the parallel group velocity would go down to zero.

In a finite temperature plasma, however, thermal effects can modify the dispersion and put an upper limit on the wave refractive index μ, while suprathermal electron populations with velocity V_{sth} can further limit the maximum μ by introducing an overwhelming Landau damping at $V_{P\parallel} \leq 2V_{sth}$ near the resonance cone angle [*Hashimoto et al.*, 1977; *Horne and Sazhin*, 1990; *Mourenas et al.*, 2014; *Li et al.*, 2014]. A rough upper bound μ_{max} corresponding to both thermal (~1–3 eV) effects and Landau damping by 100–500 eV suprathermal electrons present at $L \sim 4$–6 in the trough during moderately disturbed geomagnetic conditions is $\mu_{max} \sim \min(300, 36\Omega_{ce}/\omega)$ when Landau damping generally prevails [*Mourenas et al.*, 2014; *Li et al.*, 2014].

Above the Gendrin angle and not too far from the resonance cone, one obtains an approximate expression for the resonant electron velocity:

$$\frac{V_{R\parallel}^2}{c^2} \approx \frac{\Omega_{ce}^2}{\Omega_{pe}^2} \frac{(\cos\theta - \cos\theta_r)}{\cos\theta_r}. \tag{6}$$

from which one gets in the weakly relativistic limit $E < 20$ keV the energy E_R of electrons in Cerenkov resonance with very oblique whistler waves [*Li et al.*, 2010]:

$$E_R\ (\text{keV}) \approx \frac{250\Omega_{ce}^2}{\Omega_{pe}^2} \frac{\cos\theta - \cos\theta_r}{\cos\theta_r}. \tag{7}$$

The region $L \sim 4$–8 outside the plasmasphere corresponds in general to $\Omega_{pe}/\Omega_{ce} \sim L$ for a dipolar geomagnetic field with the (average) cold plasma density from *Sheeley et al.* [2001]. As a result, one finds resonant energies $E_R \leq 2$ keV when $\theta_m \leq \theta < \theta_r$, where θ_m is given by

$$\frac{\cos\theta_m}{\cos\theta_r} - 1 \sim \frac{L^2}{125} \tag{8}$$

or equivalently when the wave refractive index $\mu > 11\Omega_{ce}/\omega$, which is still much smaller than the above estimate for μ_{max}. Taking for instance $\omega/\Omega_{ce} = 0.34$, one finds $\theta_r \sim 70°$ and $\theta_m \sim 65°$ so that weakly damped resonance is available for $E_R \leq 2$ keV over $\Delta\theta \sim 5°$ below the resonance cone angle.

2.3. Wave-Particle Interactions Via Cyclotron Resonance

Considering very oblique waves propagating above the Gendrin angle and not too far from the resonance cone, an approximate expression for the resonant velocity $V_{R\|}$ can be similarly derived in the case of first-order cyclotron resonance:

$$\frac{V_{R\|}^2}{c^2} \simeq \frac{(\cos\theta - \cos\theta_r)(\Omega_{ce} - \omega)^2}{\cos\theta_r \cos^2\theta \Omega_{pe}^2} \tag{9}$$

from which one gets in the weakly relativistic limit $E < 30$ keV the energy E_R of electrons in first-order cyclotron resonance with very oblique whistler mode waves

$$E_R\ (\text{keV}) \approx \frac{250(\cos\theta - \cos\theta_r)(\Omega_{ce} - \omega)^2}{\cos\theta_r \cos^2\theta \Omega_{pe}^2}. \tag{10}$$

As a result, one gets low resonant electron energies $E_R \leq E_{R,\text{Max}}$(keV) when $\theta_m \leq \theta < \theta_r$ where θ_m is given by

$$\frac{\cos\theta_m}{\cos\theta_r} - 1 \approx \frac{E_{R,\text{Max}} L^2}{250} \frac{\omega^2}{(\Omega_{ce} - \omega)^2}. \tag{11}$$

or equivalently when the wave refractive index $\mu \geq (250/E_{R,\text{Max}})^{1/2}(\Omega_{ce}/\omega)(\Omega_{ce}/\omega - 1)$. Taking $E_{R,\text{Max}} = 2$ keV, the latter value is clearly larger than the value obtained from (8) in the case of Landau resonance. It remains sensibly smaller than the above estimate for $\mu_{\max}$ only for $\omega/\Omega_{ce} > 0.3$. Note that the additional presence of a beam-like distribution is expected to reduce $\mu_{\max}$ only slightly as compared with the above estimate [*Sazhin et al.*, 1990]. Taking for instance $\omega/\Omega_{ce} = 0.34$, one finds $\theta_r \sim 70°$ and $\theta_m \sim 68.5°(58°)$ for $E_{R,\text{Max}} = 2(15)$ keV. Thus, weakly damped cyclotron resonance is available for $E_R \leq 2(15)$ keV over $\Delta\theta \sim 1°(12°)$ below the resonance cone angle of lower band waves.

Comparing now cyclotron-resonant electron energies for parallel and very oblique waves, one finds

$$\frac{E_R(\theta \sim 0)}{E_{R,\text{Max}}(\theta \geq \theta_m)} \sim \frac{2\omega^2}{E_{R,\text{Max}}\Omega_{ce}^2} \frac{\Omega_{ce} - \omega}{\Omega_{ce}\cos\theta - \omega} \tag{12}$$

Equations (10)–(12) show that electron energies for cyclotron resonance are typically larger by a factor ~2 over $L \sim 5$–7 for parallel lower band chorus waves at $\omega/\Omega_{ce} \sim 0.35$ than for very oblique lower band chorus waves very close to the resonant cone angle when considering $E_{R,\text{Max}} \sim 2$ keV, but at least twice smaller for parallel waves when considering oblique lower band chorus waves farther away from the resonance cone, such that $E_R \geq 8$ keV.

Very close to Cerenkov resonance, Landau damping by Maxwellian suprathermal electrons generally becomes overwhelming, precluding efficient wave amplification via cyclotron resonance. Combining both cyclotron and Landau resonance relations shows that it occurs for $\omega/\Omega_{ce} \sim 1/2$. It is one of the possible explanations for the spectral gap usually separating lower band from upper band moderately oblique chorus waves [*Tsurutani and Smith*, 1974; *Taubenschuss et al.*, 2014].

3. Possible Scenarii for Very Oblique Whistler Mode Wave Generation

3.1. State of the Art of Whistler Mode Wave Growth in the Outer Radiation Belt

Two kinds of anisotropic electron populations have generally been observed (simultaneously or not) inside geostationary orbit (in addition to a cold isotropic population at ~ 1–3 eV): warm ($E \sim 0.3$–3 keV) and hot ($E \sim 4$–20 keV) distributions, both with temperature anisotropy $T_\perp/T_\| > 1$–2 [*Li et al.*, 2010; *Fu et al.*, 2014]. Taken together, these two distributions are able to linearly excite both parallel lower band chorus waves and more oblique upper band chorus waves, provided that the temperature anisotropies are strong enough [*Kennel and Petschek*, 1966; *Fu et al.*, 2014]. Nevertheless, average temperature anisotropies recorded by Time History of Events and Macroscale Interactions during Substorms (THEMIS) [*Li et al.*, 2010] and the Van Allen Probes [*Fu et al.*, 2014] are often too low ($T_\perp/T_\| \sim 1.5$), suggesting that spatiotemporally localized injections of more anisotropic populations are necessary to account for the generation of these waves.

When considering the above-discussed electron populations, the generation of very oblique lower band chorus waves remains elusive, in general, probably due to two facts: the much faster growth rate of parallel lower band chorus waves interacting with $E \sim 4$–15 keV anisotropic electrons [*Fu et al.*, 2014] and the high Landau damping present near the resonance cone [*Horne and Sazhin*, 1990] which likely overcomes any small growth induced by a realistic temperature anisotropy—at least when considering nearly Maxwellian distributions. Indeed, it follows from equation (10) that very oblique waves can be excited via cyclotron resonance with low-energy electrons (< 3 keV) only in the very close vicinity of the resonance cone, where significant Landau damping is present near $\mu \sim \mu_{\mathrm{max}}$. It suggests that even a strong temperature anisotropy $T_\perp/T_\parallel \sim 3$–6 might not (on its own) allow very oblique wave growth to overcome damping in this case. Considering waves generated farther away (~5°) from the resonance cone (as in THEMIS statistics from *Taubenschuss et al.* [2014]), one readily finds from equations (8) and (10)–(12) that the corresponding energy of cyclotron-resonant electrons is similar as for parallel waves. In such a situation, parallel lower band wave growth should likely overwhelm very oblique wave growth, especially as the latter waves still experience a stronger Landau damping than the former.

However, the above considerations rely on the usual assumption of a double Maxwellian shape (with different perpendicular and parallel temperatures) for the electron velocity distribution. What can happen if the latter strong assumption is actually relaxed? Since the main obstacle for the generation of very oblique whistlers is the adverse effect of Landau damping, one should examine the different parallel velocity distributions which can realistically lead to a strongly reduced (or suppressed) Landau damping.

3.2. Electron Distributions Favoring Very Oblique Lower Band Chorus Wave Growth

One first possibility which comes readily to the mind is the additional presence of a low-energy electron beam. In such a case, very oblique lower band chorus waves could actually be generated simply by inverse Landau damping for resonant velocities lying in the region of positive slope of the parallel velocity distribution. But can we expect such beam-like distributions to be present in the outer radiation belt?

Low-energy (~ 0.2–3 keV) field-aligned electron beams originating from the plasma sheet can be injected from time to time around $L \sim 7$ during substorms [e.g., see *Parks et al.*, 1977; *Reinleitner et al.*, 1983; *Klumpar et al.*, 1988; *Apatenkov et al.*, 2007, *Wang et al.*, 2014, and references therein]. Their creation involves either field-aligned electric fields or a Fermi-like acceleration in the presence of the dawn-to-dusk electric field in the plasma sheet [*Parks et al.*, 1977; *Hada et al.*, 1981; *Kan et al.*, 1988; *Shiokawa et al.*, 2003; *Apatenkov et al.*, 2007; *Wang et al.*, 2014]. Furthermore, it has recently been shown that nearly thermal electrons (~ 10–50 eV) can be directly accelerated by electrostatic structures observed by the Van Allen Probes inside the outer radiation belt [*Artemyev et al.*, 2014b; *Mozer et al.*, 2014]. The average acceleration by such localized bursts of electrostatic field has been calculated [see *Artemyev et al.*, 2014b, Figure 2(d)]. At low pitch angles, it is significantly larger for intermediate initial energies $E_0 = 25$ eV than at $E_0 = 10$ eV or $E_0 \geq 50$ eV, which may translate into a bump-on-tail velocity distribution akin to a parallel beam, with a final bump near $E_\parallel \approx 500$ eV in the considered case. Actually, moderately oblique lower band chorus waves consisting of parallel-generated waves refracting to larger θ along their propagation to higher latitudes, can themselves produce such kinds of beams by electron trapping and acceleration through Landau resonance [e.g., see *Gurnett and Reinleitner*, 1983; *Artemyev et al.*, 2012] as well as via cyclotron resonance under appropriate circumstances [e.g., see *Shklyar and Matsumoto*, 2009, and references therein].

Whatever their actual generation process, low-energy beams can sometimes be observed at $L \sim 5$ well inside the outer radiation belt [e.g., see *Kellogg et al.*, 2011] and intense field-aligned low-energy (0.2–3 keV) electron beams or streams occur frequently at $L \sim 5$–7 in the equatorial zone following substorm onset dipolarizations [*Abel et al.*, 2002]. Furthermore, small spatiotemporally localized parallel beams could well go unnoticed in general in the measured time-averaged electron distributions, especially at low energies where spacecraft potential charging can often significantly alter the measurements [*Fu et al.*, 2014]. Since the generation of parallel lower band waves via cyclotron resonance with an electron population exhibiting a temperature anisotropy already requires a localized increase of this anisotropy above the measured levels [*Fu et al.*, 2014], it does not seem unreasonable to assume that similar bursts of parallel beams may also be present, although probably more rarely.

In such a case, however, Langmuir waves should be simultaneously excited by the beam-plasma instability with a larger growth rate than oblique whistlers. The much higher frequency Langmuir waves will grow and, after reaching high enough amplitudes, they will tend to quasi-linearly flatten the beam profile, thereby reducing oblique wave growth. Nonetheless, very oblique whistlers may still be able to grow for a while before the beam structure is eventually suppressed [e.g., see *Stenzel*, 1977]. This mechanism of very oblique lower band chorus wave generation via Landau resonance is actually roughly similar (in its initial linear stage) to the generation mechanism of auroral VLF hiss by electron precipitations analyzed in details by *Maggs* [1976] and reviewed by *Labelle and Treumann* [2002]. In our case too, Langmuir waves could be first excited by relatively high-energy ($\sim$ 5 keV) electrons and saturate, turning off this high-frequency instability and allowing unimpeded growth of very oblique whistler mode waves interacting with lower energy electrons [*Ergun et al.*, 1993]. Moreover, the presence of beam and plasma inhomogeneities, and low frequency turbulence, can efficiently reduce Langmuir wave growth and strongly retard beam relaxation [e.g., see *Goldman and DuBois*, 1982; *Lin et al.*, 1986; *Krafft et al.*, 2013]. A substantial noise level ($\approx 1-5$ pT) of very oblique lower band chorus waves is expected to arise from the propagation, refraction, and magnetospheric reflection of parallel rising tone lower band chorus waves originating from other L shells [*Chen et al.*, 2013; *Breuillard et al.*, 2014]. This could enable very oblique lower band chorus waves to reach large amplitudes during one brief interaction with a sporadic electron beam. The very small parallel group velocity of oblique whistler mode waves near their resonance cone can actually allow them to grow to significant amplitudes over a reduced path length along magnetic field lines.

Combining equations (7) and (10) shows that the (parallel) resonant electron energy E_R is always smaller for Landau resonance than for cyclotron resonance when considering very oblique lower band waves such that $\omega < \Omega_{ce}/2$. E_R is also much smaller for Landau resonance with very oblique lower band waves than with quasi-parallel waves. Thus, very low energy beams should certainly excite very oblique lower band waves mainly via Landau resonance. The latter conclusion is actually supported by computer simulations: *Zhang et al.* [1993] have shown that very oblique lower band whistlers were mainly generated via Landau resonance in the case of a 7 keV parallel beam having also a temperature anisotropy, while *Sauer and Sydora* [2010] have noted that only Landau resonance remained available for oblique lower band wave growth in the case of a parallel beam with a velocity smaller than half the electron Alfven speed. Complete 2-D particle-in-cell or Vlasov simulations in an increasing geomagnetic field will be required in the future to ascertain the possibility of oblique wave amplification via inverse Landau damping by small beams, but it still remains at this date a formidable task [*Fu et al.*, 2014].

Nevertheless, the relaxation of the beam part of the distribution under the influence of simultaneously excited Langmuir and whistler mode waves should usually lead in the end to the formation of a local plateau or slightly negative power law tail in the same parallel velocity range. Such asymptotic distribution shapes should therefore be more likely to be observed. In this regard, the bumps in parallel differential energy flux $j(E)$ recorded on board CRRES at $L \sim 5-7$ [*Abel et al.*, 2002] become much smoother when considering the energy distribution $f(E) = j(E)/p^2 \sim j(E)/E$. But even the asymptotic stream-like electron distributions still correspond to a much reduced (or suppressed) Landau damping. Since inverse Landau damping is not available anymore in this case, however, one must consider cyclotron resonance instead. The free energy driving the instability must then come from a temperature anisotropy $T_\perp/T_\parallel > 2$ at $E > 2-4$ keV strong enough to allow wave growth via cyclotron resonance to overcome a very small residual Landau damping at lower parallel velocities. As noted in the previous section, the generation of very oblique whistler mode waves by cyclotron resonance indeed corresponds to electrons of higher parallel energy than for Landau resonance: typically 2–15 keV instead of 0.3–3 keV. In the remainder of this paper, both mechanisms of very oblique wave generation will be considered.

For the sake of completeness, let us mention that if a one-directional (asymmetric) tail of suprathermal particles were to be present, the fan instability could also excite (via cyclotron resonance) lower band waves confined within 1° of θ_r [e.g., see *Krafft and Volokitin*, 2006]. But only a very small portion of the observed waves could be generated this way. Moreover, small beam-like features are likely to arise at low energy during the development of this instability [*Krafft and Volokitin*, 2006], which could allow some excitation of oblique waves by inverse Landau damping. Cyclotron-resonant wave growth due to the existing temperature anisotropy should also remain quite efficient in this case.

During a sudden burst of broadband quasi-electrostatic lower band whistlers analyzed by *Maeda and Anderson* [1982], these waves showed up at a time when the temperature anisotropy did not seem to budge as compared to the preceding period, except for a slight reduction of $T_\perp/T_\parallel \leq 2.5$ at $E \sim 1-6$ keV. But if one assumes that cyclotron resonance alone was present, then the emergence of lower band waves cannot be explained by a reduced anisotropy. Rather, the latter could be an indication that small parallel electron beams were injected at that time.

3.3. Comparisons With Wave Observations

Based on the preceding analysis, the recent statistical observations on board the THEMIS satellites at $L = 5-8$ [*Li et al.*, 2013a; *Taubenschuss et al.*, 2014] of both rising and falling tone lower band chorus waves propagating near their resonance cone could be explained by the presence of either very low energy ($< 3-4$ keV) parallel beams or a low-energy electron population exhibiting both a temperature anisotropy at 3–15 keV and a non-Maxwellian tail or plateau somewhere in the range < 4 keV of parallel energies corresponding to Landau resonance with the same very oblique waves. Moreover, falling tone lower band chorus waves (about 5 times less frequent than rising tones and rarely observed together with them) are mostly seen at very large wave normal angles [*Taubenschuss et al.*, 2014]. It could be an indication that they are generated by low-energy ($< 3-4$ keV) electron beams or streams mainly at times when the temperature anisotropy is very weak at higher energies.

The similar electric and magnetic field amplitudes of both rising and falling tones near the resonance cone suggest similar nonlinear growth rates [*Taubenschuss et al.*, 2014]. Since most THEMIS measurements were performed at magnetic latitudes $\lambda < 10°$ and most of the waves propagate away from the equator [*Li et al.*, 2013a; *Kurita et al.*, 2012], at least part of these rising and falling tones are likely generated directly with high wave normal angles (as in one previous case study by *Santolík et al.* [2009]), although quasi-parallel waves can also become oblique after refraction along their propagation away from the equatorial plane [*Chen et al.*, 2013; *Agapitov et al.*, 2013]. While the nonlinear theory of parallel chorus wave growth is now well developed [e.g., see *Trakhtengerts et al.*, 2004; *Omura et al.*, 2008; *Nunn et al.*, 2009; *Demekhov*, 2011; *Katoh and Omura*, 2011; *Katoh*, 2014], the generation of quasi-electrostatic lower band chorus waves with both rising and falling tones, as well as hooks, still remains largely unexplained—although a few preliminary models have recently been proposed for falling tones [*Nunn and Omura*, 2012; *Yamaguchi et al.*, 2013; *Soto-Chavez et al.*, 2014].

A gap at $\omega \approx 0.5\Omega_{ce}$ is generally observed in parallel chorus wave spectra [*Tsurutani and Smith*, 1974], and it has also been more recently pointed out in very oblique wave spectra [*Taubenschuss et al.*, 2014]. In the latter case, it could simply stem also from strong Landau damping at $\omega \approx 0.5\Omega_{ce}$ of quasi-parallel waves initially excited by a temperature anisotropy via cyclotron resonance close to the magnetic equator. These waves should later refract to larger wave normal angles along their propagation to higher latitudes [*Chen et al.*, 2013], eventually approaching the resonance cone. If such waves represent a significant portion of the measured waves, they can easily account for the observed spectral gap. Indeed, this gap can be seen in wave occurrences and wave magnetic amplitudes, but it is not so clearly apparent in wave electric amplitudes where most of the wave energy is concentrated near the resonance cone [*Taubenschuss et al.*, 2014]. The latter point could well be another important indication that Landau damping of very oblique waves is sensibly reduced as compared with its usual level.

It is interesting to compare detailed THEMIS statistics [*Taubenschuss et al.*, 2014] of the frequency and wave normal angle distribution of very oblique chorus waves with analytical estimates based on a generation via Landau resonance with very low energy ($E \leq 2$ keV) electron beams or via cyclotron resonance with low-energy (< 2 keV or < 15 keV) electron streams possessing both a temperature anisotropy and a local plateau or tail-like parallel velocity shape. Figure 1 shows that the $(\theta, \omega/\Omega_{ce})$ parameter range of high occurrences (and intensity) of very oblique chorus waves is in reasonable agreement with the estimates $\mu < \mu_{max}$ and $\theta \geq \theta_m$ given by equation (8) for Landau resonance in the case of lower band waves, for both rising tones and falling tones. It is worth noting that the uncertainty on measured values of θ is less than 5° here [*Taubenschuss et al.*, 2014]. One can also see that the lower bound θ_m on θ from equation (11) for cyclotron resonance with $E < 2$ keV electrons is much closer to the resonance cone angle for lower band waves. Very oblique lower band waves generated through cyclotron resonance with such very low energy electrons due to a sole temperature anisotropy should therefore remain very close to θ_r. Only higher-energy electrons ($\sim 3-10$ keV) could explain by such a mechanism the high occurrences and amplitudes of very oblique waves observed down to 5°–10° below θ_r for $\omega \leq 0.35\Omega_{ce}$.

However, the lower bounds θ_m for Landau and cyclotron resonance at the same parallel energy cross each other at $\omega \sim \Omega_{ce}/2$. As concerns rising tone upper band waves, the lower limit on θ where high occurrences are obtained in THEMIS statistics is very close to the cyclotron resonance limit at 2 keV, while the upper value of θ departs from the resonance cone, decreasing rather quickly for $\omega > 0.6\Omega_{ce}$. In contrast, the distribution of falling tone upper band waves always remains within the limits imposed by Landau resonance with less than 2 keV electrons or by cyclotron resonance with less than 1 keV electrons. What can explain these features? We

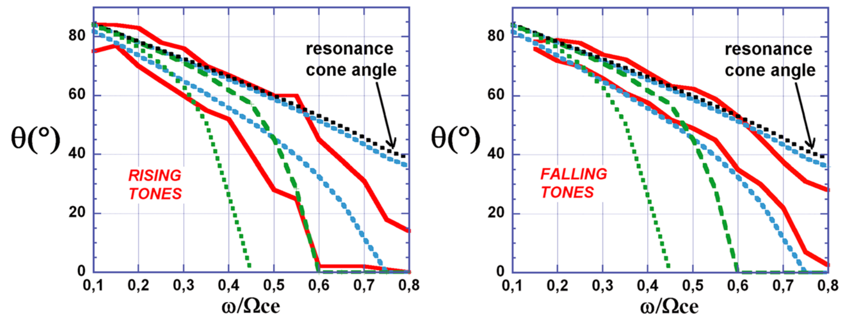

Figure 1. Distribution of very oblique chorus wave occurrences obtained in THEMIS statistics at $L \sim$5-8 (solid red curves show the limits where occurrences fall below 30% of their maximum value for a given frequency) [*Taubenschuss et al.*, 2014] and the corresponding distribution given by analytical estimates for Landau resonance with small electron beams of very low energy $E_R \leq 2$ keV (area delimited by dotted blue curves). The upper limit in analytical estimates comes from the condition $\mu < \mu_{max}$ while the lower limit corresponds to $\theta \geq \theta_m$ as given by (8) with $L \sim 7$. The corresponding lower limit for cyclotron resonance from (11) is also displayed for $E_R \leq 2$ keV and $E_R \leq 15$ keV (dashed and dotted green curves, respectively), while the resonance cone angle is plotted as a dotted black curve (in the cold plasma approximation). Rising and falling tones are displayed in left and right panels, respectively.

have already noted above that the resonant electron velocity $V_{R\parallel}$ for cyclotron resonance with very oblique waves becomes smaller than for Landau resonance when $\omega > \Omega_{ce}/2$. If a generation mechanism based on Landau resonance is operating, the competition with cyclotron resonance should reduce its efficiency at higher frequencies. If the cyclotron generation mechanism prevails, the parallel electron energy required to be in cyclotron resonance with waves close to the resonance cone angle decreases rapidly as ω increases above $\Omega_{ce}/2$. In such a case, a lower limit around 0.1–0.3 keV for strongly reduced Landau damping should lead to peak wave occurrences progressively departing from the resonance cone angle as ω increases above $\Omega_{ce}/2$, accompanied by a shift of the wave normal toward quasi-parallel propagation as in THEMIS statistics displayed in Figure 1 [*Taubenschuss et al.*, 2014].

The preceding comparisons confirm that cyclotron resonance with low-energy Maxwellian populations with temperature anisotropy probably accounts for the generation of most rising tone upper band waves at $\omega \geq 0.55\Omega_{ce}$ as well as lower band quasi-parallel waves [*Fu et al.*, 2014]. On the other hand, the proposed generation mechanisms of very oblique lower band (and falling tone upper band) waves by Landau resonance with very low energy beams or by cyclotron resonance with low-energy streams with temperature anisotropy seem to be compatible with observations and could potentially explain various features of the measured waves. However, the corresponding wave growth rates and frequency sweep rates must still be derived, which will be the subject of the next section.

4. Simplified Models of Oblique Wave Generation by Low-Energy Electron Streams

4.1. Second-Order Resonance Condition and Frequency Sweep Rates

Very oblique whistler mode waves become quasi-electrostatic near the resonance cone (for $(\Omega_{ce}\cos\theta/\omega - 1) < 0.3$), with a parallel electric field component $E_{w\parallel} \simeq E_w \cos\theta = E_{w0}\cos\theta\sin\phi$, where E_{w0} is the modulus of the field and ϕ the wave phase [*Ginzburg and Rukhadze*, 1975; *Verkhoglyadova et al.*, 2010]. The equation of motion of low-energy electrons under the influence of such a wave is given approximately by [e.g., see *Artemyev et al.*, 2012]

$$\frac{\mathrm{d}v_\parallel}{\mathrm{d}t} \simeq -\frac{v^2\sin^2\alpha}{2\Omega_{ce}}\frac{\partial\Omega_{ce}}{\partial z} - \frac{eE_{w0}\cos\theta\sin\phi}{m_e} \tag{13}$$

where m_e is the electron mass, v its velocity, and α its pitch angle.

Assuming that the first-order Cerenkov-Landau or cyclotron resonance condition is satisfied, then the derivative of the phase ϕ between the wave and the particle is given by $\mathrm{d}\phi/\mathrm{d}t = k_\parallel(v_\parallel - V_{R\parallel}) = 0$, leading to a second-order resonance condition

$$\frac{\mathrm{d}^2\phi}{\mathrm{d}t^2} = k_\parallel\frac{\mathrm{d}}{\mathrm{d}t}\left(v_\parallel - V_{R\parallel}\right). \tag{14}$$

The time derivative of the parallel resonant velocity appearing in the above equation has been calculated in Appendix A for Landau or cyclotron resonance with oblique whistler mode waves.

Using the definition of the trapping frequency $\Omega_T = \sqrt{ek_\parallel E_{w0} \cos\theta / m_e}$ of oscillations of an electron in the parallel electrostatic wave field component, one finally obtains a second-order nonlinear differential equation describing the dynamics of a resonant electron [*Omura et al.*, 2008]:

$$\frac{\mathrm{d}^2\phi}{\mathrm{d}t^2} = -\Omega_T^2 (\sin\phi + S) \tag{15}$$

where the inhomogeneity ratio S, defined as the ratio of inhomogeneity to oscillatory terms, is given by

$$\begin{aligned}\Omega_T^2 S = {} & \left(1 - \frac{V_{R\parallel}}{V_{g\parallel}}\right)^2 \frac{\partial\omega}{\partial t} \\ & + \left(\frac{\omega V_{R\parallel}\cos\theta}{2(\Omega_{\mathrm{ce}}\cos\theta - \omega)} + \frac{\omega V_{R\parallel}\tan^2\alpha}{2\Omega_{\mathrm{ce}}}\right)\frac{\partial\Omega_{\mathrm{ce}}}{\partial z}\end{aligned} \tag{16}$$

in the case of Landau resonance, while one gets for first-order cyclotron resonance:

$$\begin{aligned}\Omega_T^2 S = {} & \left(1 - \frac{V_{R\parallel}}{V_{g\parallel}}\right)^2 \frac{\partial\omega}{\partial t} \\ & + \left(\frac{k_\parallel v^2 \sin^2\alpha}{2\Omega_{\mathrm{ce}}} - \left(1 + \frac{(\Omega_{\mathrm{ce}} - \omega)\cos\theta}{2(\Omega_{\mathrm{ce}}\cos\theta - \omega)}\right) V_{R\parallel}\right)\frac{\partial\Omega_{\mathrm{ce}}}{\partial z}.\end{aligned} \tag{17}$$

The situation where electrons are decelerated and wave grows corresponds to trapping of these particles. For trapping to exist (i.e., to ensure the existence of a region of trapped particles in phase space), a necessary condition is that $|S| < 1$ [*Shklyar and Matsumoto*, 2009; *Artemyev et al.*, 2012]. Now, we assume that nonlinear growth at the equator maximizes for some (small) value S^* of $|S|$. Using equations (4) and (5) for θ near the resonance cone angle θ_r and switching to full magnetic wave amplitude B_{w0} with the help of equation (13) from *Verkhoglyadova et al.* [2010], one finds in the case of Landau resonance a frequency sweep rate

$$\frac{\partial\omega}{\partial t} \simeq \frac{\pm S^* e B_{w0}\omega^3/\Omega_{\mathrm{ce}}}{2^{1/2} m_e(\Omega_{\mathrm{ce}}\cos\theta - \omega)\left(1 - \frac{\omega}{2(\Omega_{\mathrm{ce}}\cos\theta - \omega)}\right)^2}. \tag{18}$$

Close enough to the resonance cone (i.e., at $\theta > \theta_m$ given by equation (8) for $L < 7$), equation (18) can be further approximated as

$$\frac{\partial\omega}{\partial t} \approx \pm 2^{3/2} S^* \omega^2 \left(\frac{B_{w0}}{B_0}\right)\frac{(\cos\theta - \cos\theta_r)}{\cos\theta_r}, \tag{19}$$

which shows that the modulus of the frequency sweep rate increases like $(B_{w0}/B_0)\omega^2$ at a fixed relative distance from the resonance cone angle but also that it decreases as θ gets closer to θ_r. The frequency sweep rate of very oblique lower band waves excited via Landau resonance with very low energy beams therefore varies much more quickly with the wave frequency than when considering quasi-parallel lower band chorus waves [*Omura et al.*, 2008]. For $L \sim 6$, one gets $|\partial f/\partial t| \leq S^* B_{w0}(\mathrm{pT})(f(\mathrm{kHz}))^2/25 < (B_{w0}(\mathrm{pT})/6)$ kHz/s for $\theta > \theta_m$.

In the case of cyclotron resonance, using equations (4) and (9) for θ close enough to the resonance cone angle θ_r (i.e., at $\theta > \theta_m$ given by equation (11) with $E_{R,\mathrm{Max}} \sim 10$ keV for $L < 7$), one finds similarly a frequency sweep rate

$$\frac{\partial\omega}{\partial t} \approx \pm 2^{3/2} S^* \omega^2 \left(\frac{B_{w0}}{B_0}\right)\frac{(\cos\theta - \cos\theta_r)\omega^2}{\cos\theta_r(\Omega_{\mathrm{ce}} - \omega)^2}. \tag{20}$$

Assuming a fixed wave amplitude and a sufficient energy range of instability, one can deduce from (19) and (20) that for rising tones, the frequency sweep rate should start with a relatively large value and then decrease more and more quickly as θ gets closer to the decreasing θ_r, while for falling tones the frequency sweep rate should be small initially and then increase more and more as θ further departs from the increasing θ_r. For a small enough Landau damping by the lower energy core electron population, it could produce hooks in frequency-time diagrams. But in case of a strong Landau damping by the core electron distribution (or for a narrow instability range), only rising and falling tones should be seen. In view of this rather complex behavior, it is necessary to check what can happen to the frequency sweep rate as the excited waves propagate away from the equator.

4.2. Wave Propagation Effects and Scale of the Generation Region

Following the approach of *Omura et al.* [2009], we assume here that a lower band chorus wave initially generated at $z = 0$ propagates over a distance $\Delta z = V_{g\parallel} t$ after a time t. Moreover, the derivative of the wave group velocity with respect to ω can be written as

$$\frac{\partial V_{g\parallel}}{\partial \omega} \simeq \frac{V_{g\parallel}(\Omega_{ce}\cos\theta - 4\omega)}{2\omega(\Omega_{ce}\cos\theta - \omega)}. \tag{21}$$

It shows that the group velocity has two extrema: one minimum at the resonance cone angle where it is null and a maximum for $\omega/\Omega_{ce} = \cos\theta/4$ (for $\theta = 0$, our expression (21) is equivalent to (27) in the work by *Omura et al.* [2009] in the nonrelativistic limit).

Using equations (A3) and (21), we finally get for θ close to θ_r (for both Landau and cyclotron resonances):

$$\frac{\partial \omega(t)}{\partial t} \approx \frac{1}{1 + 3\sqrt{2tS^*\omega(B_{w0}/B_0)}} \left.\frac{\partial \omega}{\partial t}\right|_{t=0}. \tag{22}$$

As a result, the frequency sweep rate can still be estimated from (19) or (20) alone as long as $t(\mathrm{s}) \ll (B_0/B_{w0})/(3 \cdot 2^{3/2}\pi S^* f)$ with f the wave frequency in hertz, or equivalently for $\Delta z \ll c(\Omega_{ce}\cos\theta/\omega - 1)^{3/2}(\Omega_{ce}/\Omega_{pe})(B_0/B_{w0})/(4\pi S^* f)$. Using (8) and $\Omega_{pe}/\Omega_{ce} \sim L$ for $\theta \simeq \theta_m$, this condition becomes $\Delta z(\mathrm{km}) \ll 5 \cdot 10^8/(LfB_{w0}S^*)$ with B_{w0} in picotesla. For $L \sim 5$ and $B_{w0} \sim 30$ pT, it is usually satisfied over at least ~ 3000 km of propagation along the magnetic field line.

It is also interesting to compare the effects of the frequency sweep rate and of the geomagnetic field variation with latitude or z in the inhomogeneity ratio S. In the case of Landau resonance, the ratio of the former term (T_f) to the latter term (T_g) on the right-hand side of equation (16) is

$$\frac{T_f}{T_g} \simeq \frac{\partial \omega}{\partial t}\left(\frac{\partial \Omega_{ce}}{\partial z}\right)^{-1} \frac{\omega \Omega_{pe}}{2c}(\Omega_{ce}\cos\theta - \omega)^{-3/2} \times \left(\omega^{1/2} + \frac{\tan^2\alpha(\Omega_{ce}\cos\theta - \omega)}{\omega^{1/2}}\right)^{-1}. \tag{23}$$

where the dipolar geomagnetic field $B(z)$ can be approximated as $B(z)/B_0 \simeq 1 + (9/2)(z/R)^2$ near the equator, with B_0 its equatorial value and $R = LR_E$ its curvature radius (R_E being Earth's radius). Consequently, the two terms T_f and T_g become equal for very oblique waves after a propagation distance z_c from the equator [*Omura et al.*, 2008]. Using (19), z_c is given by

$$z_c \simeq \frac{\sqrt{2S^*}L^2R_E^2\omega^2 B_{w0}}{9c\Omega_{ce}B_0(\Omega_{ce}\cos\theta - \omega)^{1/2}} \times \frac{\omega\Omega_{pe}}{\omega^{3/2} + \tan^2\alpha(\Omega_{ce}\cos\theta - \omega)\omega^{1/2}}. \tag{24}$$

Similarly, in the case of cyclotron resonance with electrons such that $\tan\alpha < 4$, one gets with equations (17) and (20):

$$z_c \simeq \frac{\sqrt{2S^*}L^2R_E^2\omega^{9/2}B_{w0}\Omega_{pe}}{9c\Omega_{ce}B_0(\Omega_{ce}\cos\theta - \omega)^{1/2}(\Omega_{ce} - \omega)^3}. \tag{25}$$

The maximum wave growth (with $S \simeq S^*$) can be sustained over such a distance z_c only if the wave amplitude simultaneously doubles. Thus, z_c gives a rough estimate of the dimension of the generation region. In this regard, it is interesting to note from equations (24) and (25) that z_c increases as θ gets closer to the resonance cone angle, which could partly compensate for the adverse effect of increased Landau damping by smaller-energy electrons.

Using equations (8) and (24) yields $z_c(\mathrm{km}) \sim 0.025S^*L^5f(\mathrm{kHz})B_{w0}$ (pT) for moderate pitch angle particles in Landau resonance with very oblique waves such that $\theta \simeq \theta_m$, i.e., more than 3000 km for $L \sim 5$ and $B_{w0} \sim 30$ pT when $\theta \geq \theta_m$. For cyclotron resonance, z_c is multiplied by a factor $1/(\Omega_{ce}/\omega - 1)^3 \sim 1/5$ typically, still giving more than 600 km.

Nevertheless, only parallel wave propagation and the related geomagnetic field inhomogeneity have been considered above. In reality, there will be also a transverse inhomogeneity, probably determined mainly by the transverse extent of the beam-plasma interaction region. But precise estimates of the latter inhomogeneity

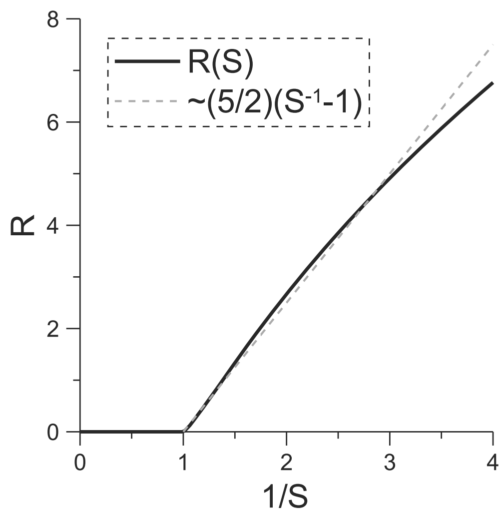

Figure 2. The function $R(S)$ (solid curve) together with the analytical fit (dashed curve).

will be hard to obtain even with modern spacecraft instruments, considering the difficulty of detecting these small low-energy beams or streams.

4.3. Nonlinear Growth Rate and the Determination of S^*

Following the approach of *Shklyar and Matsumoto* [2009], we take here into account the presence of both trapped and untrapped (transient) electron populations. In this situation, wave growth (or damping) results from energy exchanges with both transient and trapped particles. Further, assuming that the wave packet is located on one side of the equator (but very close to it) and considering asymptotic behavior (i.e., $t > 1/\Omega_T$), then the sign of the (nonlocal) nonlinear growth rate depends on the sign of the difference between energy variations of untrapped and trapped populations or equivalently on the sign of the derivative of the unperturbed population near resonance, but not on the sign of the inhomogeneity S (i.e., the nonlinear growth rate depends on S^2) [*Shklyar and Matsumoto*, 2009], leading us to use hereafter $S \equiv |S|$. Note that if only the trapped population is taken into account, the nonlinear growth rate depends linearly on S [see *Omura et al.*, 2008]. The nonlinear growth rate γ_{NL} of the wave can be defined from the ratio of change of particle energy and wave energy. Equation (4.26) from *Shklyar and Matsumoto* [2009] provides a useful general expression of γ_{NL} for whistler mode waves, based on an evaluation of the resonant current for either cyclotron or Landau resonance. This equation was examined in details by *Shklyar* [2011] in the particular case of first-order cyclotron resonance. For both Landau or first-order cyclotron resonance, this equation gives as a general expression for the nonlinear growth rate

$$\gamma_{\mathrm{NL}} = \gamma_L \frac{16}{\pi^2} \Phi^{3/2} \left\langle \Phi^{1/2} \Gamma_T S \int S(t) \mathrm{d}t \right\rangle \tag{26}$$

where γ_L is the linear growth rate, Φ is a dimensionless coefficient depending on particle energy and pitch angle (some analog to the wave-particle coupling efficiency [see *Shklyar and Matsumoto*, 2009]), Γ_T is the phase space volume of trapped particles surrounded by the separatrix of system (15), and the average is a weighted average over transverse adiabatic invariant performed with a weight $(\partial f_0/\partial W)(v_\parallel = V_{R\parallel})$, where W is the particle energy and f_0 is the distribution function of electrons. The integral inside the weighted average is performed over the time of resonant wave-particle interaction. Taking into account that resonance width is small enough in velocity space, one can approximate equation (26) as

$$\gamma_{NL} \approx \gamma_L \frac{16}{\pi^2} \Phi^2 S^2 \Gamma_T \Delta t \tag{27}$$

where Δt is the timescale of resonant interaction. The function Γ_T has a form [e.g., *Artemyev et al.*, 2012]

$$\begin{aligned} \Gamma_T &= \oint \dot{\phi} \mathrm{d}\phi \\ &= 2\Omega_T \sqrt{S} \int \sqrt{H_\phi + S^{-1} \cos\phi - \phi} \mathrm{d}\phi = 2\Omega_T \sqrt{S} R(S) \end{aligned} \tag{28}$$

where H_ϕ is the energy of the nonlinear pendulum (15). The profile of $R(S)$ is shown in Figure 2. We use the approximation $R \approx (5/2)(S^{-1} - 1)$ to obtain the final equation for γ_{NL}:

$$\gamma_{\mathrm{NL}} \approx \gamma_L \frac{80}{\pi^2} \Omega_T \Delta t \Phi^2 \left(S^{3/2} - S^{5/2} \right) \tag{29}$$

Thus, the nonlinear growth rate given by equation (29) reaches its maximum value at $S = S^* \approx 3/5$. Note also that the linear and nonlinear growth rates should reach their maximum value near the equator, due to two facts. First, the resonant velocity (6) or (9) is smaller there, allowing wave amplification by either Landau resonance with lower energy parallel beams which are generally more likely, or via cyclotron resonance with more numerous lower energy electrons. Second, the distance z_c of maximum nonlinear growth given by equations (24) or (25) is largest close to the equator where geomagnetic field inhomogeneity is smallest.

Table 1. Parameters of the Selected Cases of Intense Very Oblique Lower Band Chorus Waves, Detailing the Van Allen Probe (VAP) Spacecraft (Either A or B), Date and Time of the Observation, Location, and Local Geomagnetic Field Magnitude B_0[a]

No.	VAP	Date	UT	MLat (deg)	L	MLT	θ_{obs} (deg)	B_w (pT)	ω/Ω_{ce}	dω/dt (rad/ms)	B_0(nT)
1	B	2013-01-20	00:43:53	−6	3.9	00:30	65.7	∼50	0.45	−1.57	303
2	B	2013-01-20	00:44:56	−6	3.9	00:30	59.2	∼15	0.39	−6.29	303
3	B	2013-03-17	07:35:31	16	3.8	03:30	73.4	∼40	0.29	−10.49	638
4	B	2013-08-28	13:07:28	−0.8	5.3	18:50	77.6	∼120	0.20	−31.46	408
5	B	2013-08-28	13:07:46	−0.8	5.3	18:50	76.6	∼200	0.19	−31.60	408
6	B	2013-08-28	13:07:47	−0.8	5.3	18:50	74.3	∼120	0.21	−19.36	408
7	A	2013-03-17	09:14:11	17	3.4	05:00	74.7	∼300	0.20	+12.58	1237
8	B	2013-03-17	07:35:20	15	3.8	03:50	71.7	∼100	0.26	+52.43	638
9	B	2013-03-17	07:44:20	15	3.8	03:50	81.3	∼200	0.22	+83.89	800
10	A	2013-01-20	00:13:21	−7.7	4.3	00:00	64.3	∼70	0.22	+41.95	360
11	A	2013-01-20	00:13:21	−7.7	4.3	00:00	62.5	∼30	0.29	+18.88	360
12	B	2013-01-20	09:42:33	−5.5	4.4	01:30	71.7	∼25	0.31	+12.58	327
13	B	2013-01-20	09:42:34	−5.5	4.4	01:30	63.1	∼17.5	0.40	+13.98	327
14	B	2013-01-20	09:42:35	−5.5	4.4	01:30	55.9	∼20	0.37	+25.17	327

[a]The different wave parameters are also provided, among which the measured mean wave amplitude and frequency sweep rate (a positive one corresponds to a rising tone, a negative one to a falling tone).

4.4. Comparisons With Measured Frequency Sweep Rates

The frequency sweep rates given by equation (19) for Landau resonance and by equation (20) for cyclotron resonance (with $S^* \sim 3/5$) are strongly dependent on the exact value of the wave normal angle (i.e., on the value of $\theta - \theta_r$). Considering the limited accuracy of the determination of θ in satellite measurements (at best within $\approx \pm 2°$), this does not allow easy one-to-one direct comparisons between analytical and measured frequency sweep rates, except for selected cases where the wave normal angle is determined accurately enough. Therefore, we present here such comparisons performed using precise three-components wave magnetic and electric field measurements from the recent Van Allen Probes at $L \sim 4$–5.5, in selected cases where very oblique lower band chorus wave amplitudes are sufficiently large for the uncertainty on the exact value of θ to remain less than $\sim 2°$ to $\sim 5°$ at most.

Each of the 14 selected cases listed in Table 1 corresponds to a well-defined lower band chorus wave packet of ~ 200 ms duration on average. The precise location of each observation is provided in Table 1, together with the local time and the different wave and geomagnetic field parameters needed to estimate the wave normal angle from equations (19) and (20), as well as the measured wave normal angle. Making use of the Electric and Magnetic Field Instrument Suite and Integrated Science High Frequency Receiver (HFR) spectral data (in particular the variation of the upper hybrid frequency line) and of the variation of suprathermal electron flux given by the Helium Oxygen Proton Electron (HOPE) mass spectrometer data, these lower band chorus wave observations performed during moderately disturbed conditions have been checked to occur clearly outside of the plasmasphere (often just outside of it) in all the considered cases. The only possible exception concerns case 7 at the lowest L which could have occurred in the plasmapause transition region.

For each considered wave packet, the wave normal angle θ_{obs} has been determined using the singular value decomposition method [*Santolík et al.*, 2003], as in previous studies (e.g., see details in the works by *Agapitov et al.* [2013, 2014]). The values of θ_{obs} in Table 1 correspond to the frequency of the wave power spectral maximum. A few of the distinct wave packets listed in Table 1 have been recorded at nearly the same location within the same minute. Nevertheless, their amplitude, wave normal angle, and frequency sweep rate can be different enough. It demonstrates a significant variability in the generation process of such very oblique waves, stemming probably from the important temporal variability of the low-energy electron beams or streams which are producing them.

Most of these very oblique lower band chorus waves are observed at low magnetic latitudes within less than $\sim 5°$–$7°$ from the equatorial plane, corresponding to a distance $\Delta z \leq 2000$ km to 3000 km $\leq z_c$ from an assumed wave generation starting point located near the equator. Interestingly, however, four wave packets

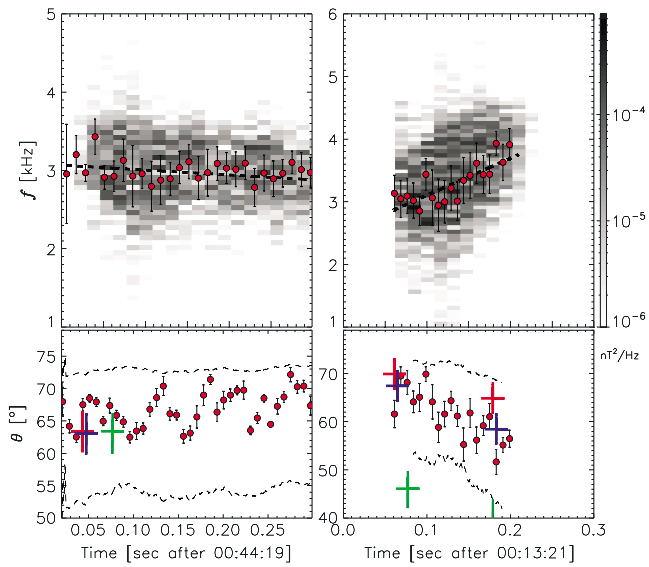

Figure 3. Very oblique lower band chorus waves measured on board the Van Allen Probe A in Earth's magnetosphere on 20 January 2013. Falling tone (left) and rising tone (right). The upper panels show the wave frequency variation as a function of time (grey shading scale indicates the wave intensity), together with the average value of the frequency corresponding to the maximum intensity (red circles with error bars). Bottom panels display the average value of the measured θ (red circles). The resonance cone angle $\theta_r = \arccos(\omega/\Omega_{ce})$ and Gendrin angle $\theta_g = \arccos(2\omega/\Omega_{ce})$ evaluated in the cold plasma approximation using the measured wave frequency and geomagnetic field strength B_0 are also plotted (upper and lower dashed lines, respectively). The inferred value of θ, allowing to recover the observed frequency sweep rate with equation (18) (resp., (19)), is displayed as a red (blue) cross in the case of Landau resonance. The inferred value of θ in the case of cyclotron resonance, as obtained from equation (20), is displayed as a green cross. For the rising tone, we show the inferred θ values both at the beginning and at the end of the time interval, because θ_r varies significantly within this interval and, as a result, the inferred θ value varies as well.

(among 14) have been recorded around 15° of magnetic latitude near dawn during one geomagnetic disturbance which moved the plasmapause location down to $L \approx 3.4$. The local geomagnetic field configuration was slightly nondipolar at that time, with a measured $B(z)$ varying from ~0.8 to ~1.11 times its dipolar value over 2 h at nearly the same location. In these four cases, it is assumed that the oblique wave generation mainly took place within less than 5° from the observation point and at lower latitudes, i.e., with a starting point near an actual nearly null gradient of $B(z)$ located within about 10° of the estimated (dipolar) magnetic equator. Although the possibility that the generation region was actually farther from the observation point (i.e., closer to the equator) cannot be totally ruled out in these four particular cases, it is worth noting that strong Landau damping outside of the generation region should then likely prevent such very oblique waves, very close to their resonance cone angle, from propagating with such high amplitudes up to the spacecraft latitude [e.g., see *Chen et al.*, 2013]. In case of a low damping, the waves could also have been generated near the equator and kept their main characteristics along propagation, provided that the weak local magnetic field inhomogeneity was somewhat reduced in this region. Still, in these four particular cases, one cannot completely exclude the possibility of a refraction of the waves to slightly higher (by a few degrees) θ values during propagation from their generation region.

Figure 3 shows two typical very oblique falling tone and rising tone lower band chorus wave packets measured near the equatorial plane. Magnetic wave amplitudes B_{w0} are around 50–150 pT and the wave normal angle is rather close to the resonance cone angle. Assuming Landau resonance excitation, the observed frequency sweep rate is fitted by a linear slope calculated with equations (18) or (19) using measured values of wave amplitude, frequency, and geomagnetic field B_0, choosing the value of the wave normal angle θ providing the best fit to the observed frequency variation. Considering also a possible wave generation via cyclotron resonance, the same procedure is repeated using equation (20) for the corresponding frequency sweep rate. Then, the corresponding inferred θ values can be compared with the value of θ *measured* by the Van Allen Probes. Analytical and mean measured θ values appear to be quite close in these two cases when assuming Landau resonance. A good agreement is also obtained for the falling tone (but not for the rising tone) when assuming cyclotron resonance.

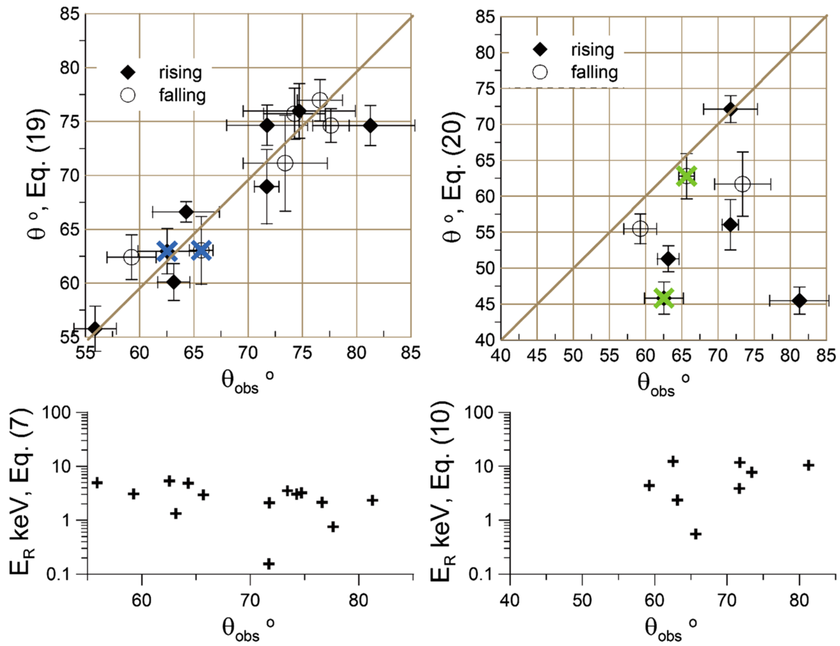

Figure 4. Comparisons between the mean observed wave normal angle θ_{obs} of very oblique lower band chorus waves and the value of θ inferred with the help of analytical expressions (19) for Landau resonance (left) and (20) for cyclotron resonance (right) of the frequency sweep rate on the basis of the wave amplitude, frequency, and geomagnetic field strength measured by the Van Allen Probes near the equator. Both rising tones (diamonds) and falling tones (empty circles) very oblique waves are considered. Error bars show the uncertainties related to the averaging performed over varying measured parameters (wave frequency, intensity, wave normal angle, geomagnetic field strength). Blue and green crosses show two events from Figure 3. The corresponding parallel energy E_R of resonant electrons is plotted in the lower panels, as calculated from equations (7) and (10) using a mean ratio $\Omega_{pe}/\Omega_{ce} \sim 5$ corresponding to our data set in the region $L \sim 5$. The inferred θ values (very close to the observed ones) are used when considering Landau resonance, while observed values are used in the case of cyclotron resonance.

More comparisons between the mean value of the measured wave normal angle θ of very oblique lower band chorus waves and its value inferred from analytical expressions (19) and (20) are displayed in Figure 4 for other similar observations on board the Van Allen Probes. One can see that the inferred θ most often remains within less than $\sim$ 3° from the mean value of the measured wave normal angle when using equation (19) corresponding to Landau resonance. Thus, the analytical estimates of the frequency sweep rate obtained under the assumption of a wave generation mechanism involving Landau resonance with a low-energy (< 4 keV) electron beam are in good agreement with observations in these selected cases. It shows that at least some of the observed very oblique lower band chorus waves could really be generated this way near the equator.

Nevertheless, some lower band chorus wave packets could also be explained by cyclotron resonance with parallel streams of low-energy electrons exhibiting a temperature anisotropy. However, it seems to concern mainly less oblique lower band chorus waves farther from the resonance cone angle and interacting with higher-energy electrons (~10 keV), as in previous studies considering quasi-parallel waves [*Omura et al.*, 2008; *Fu et al.*, 2014]. As the size z_c of the generation region is sensibly smaller for a cyclotron resonance mechanism than for Landau resonance, some of the observations might have been performed too far from a cyclotron resonance generation region to yield a good agreement with theoretical estimates. In the future, it would be interesting also to undertake further comparisons between the observed frequency sweep rates and sweep rates calculated on the basis of the nonlinear Backward wave oscillator theory [*Trakhtengerts et al.*, 2004; *Demekhov*, 2011] adapted for very oblique waves, which could lead to a better agreement in the case of cyclotron resonance.

5. Discussion and Conclusion

The possibility of very oblique lower band chorus wave generation by means of Landau resonance interaction with unstable low-energy electron beams or by cyclotron resonance with anisotropic low-energy streams has been examined above from a theoretical point of view and then compared to various satellite observations. The distribution of measured very oblique waves near the equator in the (ω, θ) domain [*Taubenschuss et al.*, 2014] has been found to compare well with expectations based on Landau resonance with sporadic very low energy (< 2–4 keV) electron beams injected from the plasma sheet or produced in situ. An alternative generation mechanism based on cyclotron resonance with an electron population exhibiting a sufficient temperature anisotropy at low-energy (∼ 1–15 keV) together with a local plateau or power law tail in its parallel velocity distribution at still lower energies corresponding to Landau resonance with the same very oblique waves would lead to an (ω, θ) distribution in much less good agreement with observations when considering only very low energy (≤ 2 keV) particles but comes closer to the observations when allowing higher-energy (2–15 keV) electrons. The fact that rising and falling tone very oblique waves exhibit similar levels of, and ratios of, magnetic and electric field amplitudes lends support to the hypothesis of a similar generation process with a common source region located near the equator [*Taubenschuss et al.*, 2014].

It is a much more difficult task to compare precisely the observed frequency sweep rates of very oblique lower band chorus wave packets with the corresponding analytical expressions obtained for Landau and cyclotron resonances. Nevertheless, analytical estimates obtained under the assumption of Landau resonance with small beams have been shown to be in good agreement with average measured values in at least a number of cases carefully selected for the good accuracy of the wave normal angle measurements on board the Van Allen Probes close to the equator. Only a small portion of our observations could apparently be explained by assuming cyclotron resonance. While this confirms the compatibility of the Landau resonance wave generation mechanism with observations, more numerous (statistical) comparisons would nevertheless be needed to ascertain the relative importance of this mechanism as compared with the other one based on cyclotron resonance with electron streams having a temperature anisotropy. But such a comprehensive study is beyond the scope of the present paper and left for a future dedicated work.

The characteristic scale length of the corresponding generation region of very oblique lower band chorus waves is typically ∼ 1000 km (for cyclotron resonance) to 3000 km (for Landau resonance) along magnetic field lines on both sides of the equator. It would be interesting in next studies to compare this estimate with satellite observations, as well as to try to evaluate the transverse scale of the generation region. The latter might indeed impose additional constraints to the proposed generation mechanisms, due to the partly transverse propagation of the oblique waves. In the inner magnetosphere, most very oblique lower band waves are observed in regions of relatively low ratio $\Omega_{pe}/\Omega_{ce} < 5.5$ [*Li et al.*, 2012; *Taubenschuss et al.*, 2014], which corresponds to $L \sim 5$ just outside the plasmasphere. At higher L shells, parallel resonant energies for both cyclotron and Landau resonance with very oblique waves decrease with the ratio $\Omega^2_{ce}/\Omega^2_{pe} \sim 1/L^2$. It means that inverse (or at least reduced) Landau damping (as well as temperature anisotropy) is required to exist at lower parallel energies, closer to the dense core of Maxwellian electrons injected from the plasma sheet. This becomes probably less easy, in general, as one draws closer to the magnetopause.

Some high-frequency waves can be noticed near the electron plasma frequency in the electric field data of the Van Allen Probes at the same time as very oblique lower band chorus waves are observed. The simultaneous generation of Langmuir waves would lend further credence to the presence of an electron beam. However, it is often difficult to unambiguously distinguish Langmuir waves from nearby electrostatic Bernstein waves excited by temperature or loss cone anisotropies at higher energy [e.g., see *Mourenas and Beghin*, 1991]. Further investigations are therefore necessary to examine this possibility.

Finally, only simultaneous experimental observations of these very oblique lower band chorus waves together with small low-energy electron beams or streams could definitely establish the effectiveness of these generation processes inside the magnetosphere. But it remains to this day a very challenging goal.

Appendix A: Velocity at Landau or Cyclotron Resonance as Seen by an Electron

Based on usual definitions of wave phase, wave number, and frequency and assuming slowly varying wave phase, amplitude, ω, k, and wave normal angle θ, as a function of time and position z along the magnetic field line, we have

$$\frac{\partial k_\parallel}{\partial t} = -\frac{\partial \omega}{\partial z}. \tag{A1}$$

while differentiation of the oblique whistler mode dispersion relation with respect to time leads to

$$2c^2 k \frac{\partial k}{\partial t} \simeq -\frac{\Omega_{ce}\Omega_{pe}^2 \cos\theta}{(\Omega_{ce}\cos\theta-\omega)^2}\frac{\partial\omega}{\partial t}. \tag{A2}$$

From (3), (A1), and (A2), one gets the propagation equation for the wave frequency:

$$\frac{\partial\omega}{\partial t} + V_{g\parallel}\frac{\partial\omega}{\partial z} = 0. \tag{A3}$$

Differentiating the dispersion relation with respect to position z (assuming for simplicity a constant density) and using (3) and (A1), one obtains a similar propagation equation for $k_\parallel$:

$$\frac{\partial k_\parallel}{\partial z} = -\frac{1}{V_{g\parallel}}\frac{\partial k_\parallel}{\partial t} - \frac{\Omega_{pe}\omega^{1/2}\cos^2\theta}{2c(\Omega_{ce}\cos\theta-\omega)^{3/2}}\frac{\partial\Omega_{ce}}{\partial z}. \tag{A4}$$

Since we are dealing with oblique wave growth and propagation over only a very small path length along magnetic field lines (corresponding to $\Delta\lambda \le 2°$), wave refraction is likely negligible, justifying the assumption of a constant wave normal angle θ used throughout the present study. Now, the time variation of the frequency ω seen by a particle moving at a parallel velocity $v_\parallel$ is

$$\frac{\mathrm{d}\omega}{\mathrm{d}t} = \frac{\partial\omega}{\partial t} + v_\parallel\frac{\partial\omega}{\partial z} = \left(1-\frac{v_\parallel}{V_{g\parallel}}\right)\frac{\partial\omega}{\partial t}. \tag{A5}$$

Making use of equation (A4), the temporal variation of $k_\parallel$ seen by the same particle is

$$\frac{\mathrm{d}k_\parallel}{\mathrm{d}t} = \left(1-\frac{v_\parallel}{V_{g\parallel}}\right)\frac{\partial k_\parallel}{\partial t} - \frac{v_\parallel\Omega_{pe}\omega^{1/2}\cos^2\theta}{2c(\Omega_{ce}\cos\theta-\omega)^{3/2}}\frac{\partial\Omega_{ce}}{\partial z}. \tag{A6}$$

On this basis, we can now derive two equations for the temporal evolution of the resonant velocity $V_{R\parallel}$ as seen by an electron in either Landau or cyclotron resonance with an oblique lower band chorus wave, in a fashion similar to the work by *Omura et al.* [2008] for parallel chorus nonlinear wave growth in the case of cyclotron resonance. Replacing equations (A5) and (A6) in the expression $\mathrm{d}V_{R\parallel}/\mathrm{d}t = (1/k_\parallel)\mathrm{d}\omega/\mathrm{d}t - (\omega/k_\parallel^2)\mathrm{d}k_\parallel/\mathrm{d}t$ valid in the nonrelativistic limit, one obtains for Landau resonance:

$$\begin{aligned}\frac{\mathrm{d}V_{R\parallel}}{\mathrm{d}t} &= \frac{1}{k_\parallel}\left(1-\frac{V_{R\parallel}}{V_{g\parallel}}\right)\left(1-\frac{v_\parallel}{V_{g\parallel}}\right)\frac{\partial\omega}{\partial t}\\ &\quad+\frac{v_\parallel\omega\cos\theta}{2k_\parallel(\Omega_{ce}\cos\theta-\omega)}\frac{\partial\Omega_{ce}}{\partial z}.\end{aligned} \tag{A7}$$

while using $\mathrm{d}\Omega_{ce}/\mathrm{d}t = v_\parallel\partial\Omega_{ce}/\partial z$, one gets for first-order cyclotron resonance

$$\begin{aligned}\frac{\mathrm{d}V_{R\parallel}}{\mathrm{d}t} &= \frac{1}{k_\parallel}\left(1-\frac{V_{R\parallel}}{V_{g\parallel}}\right)\left(1-\frac{v_\parallel}{V_{g\parallel}}\right)\frac{\partial\omega}{\partial t}\\ &\quad-\frac{v_\parallel}{k_\parallel}\left(1+\frac{(\Omega_{ce}-\omega)\cos\theta}{2(\Omega_{ce}\cos\theta-\omega)}\right)\frac{\partial\Omega_{ce}}{\partial z}.\end{aligned} \tag{A8}$$

Acknowledgments
The work of O.A. and F.M. was supported in part by NSF grants AGS1202330 and AGS1219369 and JHU/APL contract 922613 (RBSP-EFW). The work of A.V.A. was also partially supported by the grant MK-1781.2014.2. All data used in this paper can be found at RBSP/EFW database (http://www.space.umn.edu/missions/rbspefw-home-university-of-minnesota/)

Michael W. Liemohn thanks the reviewers for their assistance in evaluating this paper.

References

Abel, G. A., A. N. Fazakerley, and A. D. Johnstone (2002), Statistical distributions of field-aligned electron events in the near-equatorial magnetosphere observed by the Low Energy Plasma Analyzer on CRRES, *J. Geophys. Res.*, *107*(A11), 1393, doi:10.1029/2001JA005073.

Agapitov, O., V. Krasnoselskikh, Y. Zaliznyak, V. Angelopoulos, O. Le Contel, and G. Rolland (2010), Chorus source region localization in the Earth outer magnetosphere using THEMIS measurements, *Ann. Geophys.*, *28*, 1377–1386, doi:10.5194/angeo-28-1377-2010.

Agapitov, O., A. Artemyev, V. Krasnoselskikh, Y. V. Khotyaintsev, D. Mourenas, H. Breuillard, M. Balikhin, and G. Rolland (2013), Statistics of whistler mode waves in the outer radiation belt: Cluster STAFF-SA measurements, *J. Geophys. Res. Space Physics*, *118*, 3407–3420, doi:10.1002/jgra.50312.

Agapitov, O., A. Artemyev, D. Mourenas, V. Krasnoselskikh, J. Bonnell, O. Le Contel, C. M. Cully, and V. Angelopoulos (2014), The quasi-electrostatic mode of chorus waves and electron nonlinear acceleration, *J. Geophys. Res. Space Physics*, *119*, 1606–1626, doi:10.1002/2013JA019223.

Albert, J. M. (2002), Nonlinear interaction of outer zone electrons with VLF waves, *Geophys. Res. Lett.*, *29*(8), 1275, doi:10.1029/2001GL013941.

Apatenkov, S. V., et al. (2007), Multi-spacecraft observation of plasma dipolarization/injection in the inner magnetosphere, *Ann. Geophys.*, *25*, 801–814, doi:10.5194/angeo-25-801-2007.

Artemyev, A., V. Krasnoselskikh, O. Agapitov, D. Mourenas, and G. Rolland (2012), Non-diffusive resonant acceleration of electrons in the radiation belts, *Phys. Plasmas*, *19*(12), 122901, doi:10.1063/1.4769726.

Artemyev, A. V., O. Agapitov, D. Mourenas, V. Krasnoselskikh, and L. Zelenyi (2013a), Storm-induced energization of radiation belt electrons: Effect of wave obliquity, *Geophys. Res. Lett.*, *40*, 4138–4143, doi:10.1002/grl.50837.

Artemyev, A. V., A. A. Vasiliev, D. Mourenas, O. V. Agapitov, and V. V. Krasnoselskikh (2013b), Nonlinear electron acceleration by oblique whistler waves: Landau resonance vs. cyclotron resonance, *Phys. Plasmas*, *20*(12), 122901, doi:10.1063/1.4836595.

Artemyev, A. V., A. A. Vasiliev, D. Mourenas, O. Agapitov, V. Krasnoselskikh, D. Boscher, and G. Rolland (2014a), Fast transport of resonant electrons in phase space due to nonlinear trapping by whistler waves, *Geophys. Res. Lett.*, *41*, 5727–5733, doi:10.1002/2014GL061380.

Artemyev, A. V., O. Agapitov, F. Mozer, and V. Krasnoselskikh (2014b), Thermal electron acceleration by localized bursts of electric field in the radiation belts, *Geophys. Res. Lett.*, *41*, 5734–5739, doi:10.1002/2014GL061248.

Bell, T. F. (1984), The nonlinear gyroresonance interaction between energetic electrons and coherent VLF waves propagating at an arbitrary angle with respect to the Earth's magnetic field, *J. Geophys. Res.*, *89*(A2), 905–918, doi:10.1029/JA089iA02p00905.

Bell, T. F., U. S. Inan, N. Haque, and J. S. Pickett (2009), Source regions of banded chorus, *Geophys. Res. Lett.*, *36*, L11101, doi:10.1029/2009GL037629.

Breuillard, H., O. Agapitov, A. Artemyev, V. Krasnoselskikh, O. Le Contel, C. M. Cully, V. Angelopoulos, Y. Zaliznyak, and G. Rolland (2014), On the origin of falling-tone chorus elements in Earth's inner magnetosphere, *Ann. Geophys.*, *32*, 1477–1485, doi:10.5194/angeo-32-1477-2014.

Burtis, W. J., and R. A. Helliwell (1969), Banded chorus—A new type of VLF radiation observed in the magnetosphere by Ogo 1 and Ogo 3, *J. Geophys. Res.*, *74*(11), 3002–3010, doi:10.1029/JA074i011p03002.

Burtis, W. J., and R. A. Helliwell (1976), Magnetospheric chorus: Occurrence patterns and normalized frequency, *Planet. Space Sci.*, *24*(11), 1007–1024, doi:10.1016/0032-0633(76)90119-7.

Cattell, C., et al. (2008), Discovery of very large amplitude whistler-mode waves in Earth's radiation belts, *Geophys. Res. Lett.*, *35*, L01105, doi:10.1029/2007GL032009.

Chen, L., R. M. Thorne, W. Li, and J. Bortnik (2013), Modeling the wave normal distribution of chorus waves, *J. Geophys. Res. Space Physics*, *118*, 1074–1088, doi:10.1029/2012JA018343.

Chen, Y., G. D. Reeves, R. H. W. Friedel, and G. S. Cunningham (2014), Global time-dependent chorus maps from low-Earth-orbit electron precipitation and Van Allen Probes data, *Geophys. Res. Lett.*, *41*, 755–761, doi:10.1002/2013GL059181.

Cully, C. M., J. W. Bonnell, and R. E. Ergun (2008), THEMIS observations of long-lived regions of large-amplitude whistler waves in the inner magnetosphere, *Geophys. Res. Lett.*, *35*, L17S16, doi:10.1029/2008GL033643.

Cully, C. M., V. Angelopoulos, U. Auster, J. Bonnell, and O. Le Contel (2011), Observational evidence of the generation mechanism for rising tone chorus, *Geophys. Res. Lett.*, *38*, L01106, doi:10.1029/2010GL045793.

Demekhov, A. G. (2011), Generation of VLF emissions with the increasing and decreasing frequency in the magnetosperic cyclotron maser in the backward wave oscillator regime, *Radiophys. Quantum Electron.*, *53*(11), 609–622, doi:10.1007/s11141-011-9256-x.

Ergun, R. E., G. T. Delory, E. Klementis, C. W. Carlson, J. P. McFadden, I. Roth, and M. Temerin (1993), VLF wave growth from dispersive bursts of field-aligned electron fluxes, *J. Geophys. Res.*, *98*, 3777–3787, doi:10.1029/92JA02193.

Fu, X., et al. (2014), Whistler anisotropy instabilities as the source of banded chorus: Van Allen Probes observations and particle-in-cell simulations, *J. Geophys. Res. Space Physics*, *119*, 8288–8298, doi:10.1002/2014JA020364.

Ginzburg, V. L., and A. A. Rukhadze (1975), *Waves in Magnetoactive Plasma*, 2nd rev. ed., Nauka Ed., Moscow.

Goldman, M. V., and D. F. DuBois (1982), Beam plasma instability in the presence of low frequency turbulence, *Phys. Fluids*, *25*, 1062–1072, doi:10.1063/1.863839.

Gurnett, D. A., and L. A. Reinleitner (1983), Electron acceleration by Landau resonance with whistler mode wave packets, *Geophys. Res. Lett.*, *10*, 603–606, doi:10.1029/GL010i008p00603.

Hada, T., A. Nishida, T. Teresawa, and E. W. Hones Jr. (1981), Bi-directional electron pitch angle anisotropy in the plasma sheet, *J. Geophys. Res.*, *86*(A13), 11,211–11,224, doi:10.1029/JA086iA13p11211.

Hashimoto, K., I. Kimura, and H. Kumagai (1977), Estimation of electron temperature by VLF waves propagating in directions near the resonance cone, *Planet. Space Sci.*, *25*, 871–877.

Hayakawa, M., Y. Yamanaka, M. Parrot, and F. Lefeuvre (1984), The wave normals of magnetospheric chorus emissions observed on board GEOS 2, *J. Geophys. Res.*, *89*, 2811–2821, doi:10.1029/JA089iA05p02811.

Horne, R. B., and S. S. Sazhin (1990), Quasielectrostatic and electrostatic approximations for whistler mode waves in the magnetospheric plasma, *Planet. Space Sci.*, *38*(2), 311–318.

Horne, R. B., et al. (2005), Wave acceleration of electrons in the Van Allen radiation belts, *Nature*, *437*, 227–230, doi:10.1038/nature03939.

Inan, U. S., and T. F. Bell (1991), Pitch angle scattering of energetic particles by oblique whistler waves, *Geophys. Res. Lett.*, *18*(1), 49–52, doi:10.1029/90GL02476.

Kan, J. R., L. Zhu, and S.-I. Akasofu (1988), A theory of substorms: Onset and subsidence, *J. Geophys. Res.*, *93*(A6), 5624–5640, doi:10.1029/JA093iA06p05624.

Karpman, V. I., J. N. Istomin, and D. R. Shklyar (1974), Nonlinear frequency shift and self-modulation of the quasi-monochromatic whistlers in the inhomogeneous plasma (magnetosphere), *Planet. Space Sci.*, *22*, 859–871, doi:10.1016/0032-0633(74)90155-X.

Katoh, Y., and Y. Omura (2011), Amplitude dependence of frequency sweep rates of whistler mode chorus emissions, *J. Geophys. Res.*, *116*, A07201, doi:10.1029/2011JA016496.

Katoh, Y. (2014), A simulation study of the propagation of whistler-mode chorus in the Earth's inner magnetosphere, *Earth Planets Space*, *66*, 6, doi:10.1186/1880-5981-66-6.

Kellogg, P. J., C. A. Cattell, K. Goetz, S. J. Monson, and L. B. Wilson III (2011), Large amplitude whistlers in the magnetosphere observed with Wind-Waves, *J. Geophys. Res.*, *116*, A09224, doi:10.1029/2010JA015919.

Kennel, C. F., and H. E. Petschek (1966), Limit on stably trapped particle fluxes, *J. Geophys. Res.*, *71*, 1–28.

Klumpar, D. M., J. M. Quinn, and E. G. Shelley (1988), Counterstreaming electrons at the magnetic equator near 9 R_E, *Geophys. Res. Lett.*, *15*, 1295–1298, doi:10.1029/GL015i011p01295.

Krafft, C., and A. Volokitin (2006), Stabilization of the fan instability: Electron flux relaxation, *Phys. Plasmas*, *13*(12), 122301, doi:10.1063/1.2372464.

Krafft, C., A. S. Volokitin, and V. V. Krasnoselskikh (2013), Interaction of energetic particles with waves in strongly inhomogeneous solar wind plasmas, *Astrophys. J.*, *778*, 111–122, doi:10.1088/0004-637X/778/2/111.

Kurita, S., H. Misawa, C. M. Cully, O. Le Contel, and V. Angelopoulos (2012), Source location of falling tone chorus, *Geophys. Res. Lett.*, *39*, L22102, doi:10.1029/2012GL053929.

Labelle, J., and R. A. Treumann (2002), Auroral Radio emissions, hisses, roars, and bursts, *Space Sci. Rev.*, *101*, 295–440, doi:10.1023/A:1020850022070.

LeDocq, M. J., D. A. Gurnett, and G. B. Hospodarsky (1998), Chorus source locations from VLF Poynting flux measurements with the Polar spacecraft, *Geophys. Res. Lett.*, *25*(21), 4063–4066, doi:10.1029/1998GL900071.

Li, W., et al. (2010), THEMIS analysis of observed equatorial electron distributions responsible for the chorus excitation, *J. Geophys. Res.*, *115*, A00F11, doi:10.1029/2009JA014845.

Li, W., R. M. Thorne, J. Bortnik, X. Tao, and V. Angelopoulos (2012), Characteristics of hiss-like and discrete whistler-mode emissions, *Geophys. Res. Lett.*, *39*, L18106, doi:10.1029/2012GL053206.

Li, W., J. Bortnik, R. M. Thorne, C. M. Cully, L. Chen, V. Angelopoulos, Y. Nishimura, J. B. Tao, J. W. Bonnell, and O. Le Contel (2013a), Characteristics of the Poynting flux and wave normal vectors of whistler-mode waves observed on THEMIS, *J. Geophys. Res. Space Physics*, *118*, 1461–1471, doi:10.1002/jgra.50176.

Li, W., B. Ni, R. M. Thorne, J. Bortnik, J. C. Green, C. A. Kletzing, W. S. Kurth, and G. B. Hospodarsky (2013b), Constructing the global distribution of chorus wave intensity using measurements of electrons by the POES satellites and waves by the Van Allen Probes, *Geophys. Res. Lett.*, *40*, 4526–4532, doi:10.1002/grl.50920.

Li, W., et al. (2014), Evidence of stronger pitch angle scattering loss caused by oblique whistler-mode waves as compared with quasi-parallel waves, *Geophys. Res. Lett.*, *41*, 6063–6070, doi:10.1002/2014GL061260.

Lin, R. P., W. K. Levedahl, W. Lotko, D. A. Gurnett, and F. L. Scarf (1986), Evidence for nonlinear wave-wave interactions in solar type III radio bursts, *Astrophys. J.*, *308*, 954–965, doi:10.1086/164563.

Lyons, L. R. (1974), Pitch angle and energy diffusion coefficients from resonant interactions with ion-cyclotron and whistler waves, *J. Plasma Phys.*, *12*, 417–432, doi:10.1017/S002237780002537X.

Lyons, L. R., R. M. Thorne, and C. F. Kennel (1972), Pitch-angle diffusion of radiation belt electrons within the plasmasphere, *J. Geophys. Res.*, *77*, 3455–3474, doi:10.1029/JA077i019p03455.

Maeda, K., and R. R. Anderson (1982), A broadband VLF burst associated with ring current electrons, *J. Geophys. Res.*, *87*(A11), 9120–9128, doi:10.1029/JA087iA11p09120.

Maggs, J. E. (1976), Coherent generation of VLF hiss, *J. Geophys. Res.*, *81*(10), 1707–1724, doi:10.1029/JA081i010p01707.

Meredith, N. P., R. B. Horne, A. Sicard-Piet, D. Boscher, K. H. Yearby, W. Li, and R. M. Thorne (2012), Global model of lower band and upper band chorus from multiple satellite observations, *J. Geophys. Res.*, *117*, A10225, doi:10.1029/2012JA017978.

Mourenas, D., and C. Beghin (1991), Packets of cyclotron waves induced by electron beam injection from the space shuttle 1. Linear theory, *Radio Sci.*, *26*, 469–479, doi:10.1029/90RS02580.

Mourenas, D., A. V. Artemyev, J.-F. Ripoll, O. V. Agapitov, and V. V. Krasnoselskikh (2012a), Timescales for electron quasi-linear diffusion by parallel and oblique lower-band Chorus waves, *J. Geophys. Res.*, *117*, A06234, doi:10.1029/2012JA017717.

Mourenas, D., A. V. Artemyev, O. V. Agapitov, and V. V. Krasnoselskikh (2012b), Acceleration of radiation belts electrons by very oblique chorus waves, *J. Geophys. Res.*, *117*, A10212, doi:10.1029/2012JA018041.

Mourenas, D., A. Artemyev, O. Agapitov, and V. Krasnoselskikh (2014), Consequences of geomagnetic activity on energization and loss of radiation belt electrons by oblique chorus waves, *J. Geophys. Res. Space Physics*, *119*, 2775–2796, doi:10.1002/2013JA019674.

Mozer, F. S., S. D. Bale, J. W. Bonnell, C. C. Chaston, I. Roth, and J. Wygant (2013), Megavolt parallel potentials arising from double-layer streams in the Earth's outer radiation belt, *Phys. Rev. Lett.*, *111*(23), 235002, doi:10.1103/PhysRevLett.111.235002.

Mozer, F. S., O. Agapitov, V. Krasnoselskikh, S. Lejosne, G. D. Reeves, and I. Roth (2014), Direct observation of radiation belt electron acceleration from electron volt energies to megavolts by non-linear whistlers, *Phys. Rev. Lett.*, *113*, 035001.

Nunn, D. (1971), A theory of VLF emissions, *Planet. Space Sci.*, *19*, 1141–1167, doi:10.1016/0032-0633(71)90110-3.

Nunn, D., O. Santolik, M. Rycroft, and V. Trakhtengerts (2009), On the numerical modelling of VLF chorus dynamical spectra, *Ann. Geophys.*, *27*, 2341–2359, doi:10.5194/angeo-27-2341-2009.

Nunn, D., and Y. Omura (2012), A computational and theoretical analysis of falling frequency VLF emissions, *J. Geophys. Res.*, *117*, A08228, doi:10.1029/2012JA017557.

Omura, Y., Y. Katoh, and D. Summers (2008), Theory and simulation of the generation of whistler-mode chorus, *J. Geophys. Res.*, *113*, A04223, doi:10.1029/2007JA012622.

Omura, Y., M. Hikishima, Y. Katoh, D. Summers, and S. Yagitani (2009), Nonlinear mechanisms of lower-band and upper-band VLF chorus emissions in the magnetosphere, *J. Geophys. Res.*, *114*, A07217, doi:10.1029/2009JA014206.

Orlova, K., and Y. Shprits (2014), Model of lifetimes of the outer radiation belt electrons in a realistic magnetic field using realistic chorus wave parameters, *J. Geophys. Res. Space Physics*, *119*, 770–780, doi:10.1002/2013JA019596.

Osmane, A., and A. M. Hamza (2014), Relativistic surfatron process for Landau resonant electrons in radiation belts, *Nonlinear Processes Geophys.*, *21*, 115–125, doi:10.5194/npg-21-115-2014.

Parks, G. K., C. S. Lin, B. Mauk, S. DeForrest, and C. E. McIlwain (1977), Characteristics of magnetospheric particle injection deduced from events observed on August 18, 1974, *J. Geophys. Res.*, *82*(32), 5208–5214, doi:10.1029/JA082i032p05208.

Reinleitner, L. A., D. A. Gurnett, and T. E. Eastman (1983), Electrostatic bursts generated by electrons in Landau Resonance with whistler mode chorus, *J. Geophys. Res.*, *88*(A4), 3079–3093, doi:10.1029/JA088iA04p03079.

Santolík, O., M. Parrot, and F. Lefeuvre (2003), Singular value decomposition methods for wave propagation analysis, *Radio Sci.*, *38*(1), 1010, doi:10.1029/2000RS002523.

Santolík, O., D. A. Gurnett, J. S. Pickett, M. Parrot, and N. Cornilleau-Wehrlin (2005), Central position of the source region of storm-time chorus, *Planet. Space Sci.*, *53*(1), 299–305, doi:10.1016/j.pss.2004.09.056.

Santolík, O., D. A. Gurnett, J. S. Pickett, J. Chum, and N. Cornilleau-Wehrlin (2009), Oblique propagation of whistler mode waves in the chorus source region, *J. Geophys. Res.*, *114*, A00F03, doi:10.1029/2009JA014586.

Sauer, K., and R. D. Sydora (2010), Beam-excited whistler waves at oblique propagation with relation to STEREO radiation belt observations, *Ann. Geophys.*, *28*, 1317–1325, doi:10.5194/angeo-28-1317-2010.

Sazhin, S. S., S. N. Walker, and L. J. C. Woolliscroft (1990), Oblique whistler-mode waves in the presence of electron beams, *Planet. Space Sci.*, *38*, 791–805, doi:10.1016/0032-0633(90)90038-R.

Sheeley, B. W., M. B. Moldwin, H. K. Rassoul, and R. R. Anderson (2001), An empirical plasmasphere and trough density model: CRRES observations, *J. Geophys. Res.*, *106*, 25,631–25,642, doi:10.1029/2000JA000286.

Shiokawa, K., W. Baumjohann, and G. Paschmann (2003), Bi-directional electrons in the near-Earth plasma sheet, *Ann. Geophys.*, *21*, 1497–1507, doi:10.5194/angeo-21-1497-2003.

Shklyar, D., and H. Matsumoto (2009), Oblique whistler-mode waves in the inhomogeneous magnetospheric plasma: Resonant interactions with energetic charged particles, *Surv. Geophys.*, *30*, 55–104, doi:10.1007/s10712-009-9061-7.

Shklyar, D. R. (2011), On the nature of particle energization via resonant wave-particle interaction in the inhomogeneous magnetospheric plasma, *Ann. Geophys.*, *29*, 1179–1188, doi:10.5194/angeo-29-1179-2011.

Soto-Chavez, A. R., G. Wang, A. Bhattacharjee, G. Y. Fu, and H. M. Smith (2014), A model for falling-tone chorus, *Geophys. Res. Lett.*, *41*, 1838–1845, doi:10.1002/2014GL059320.

Stenzel, R. (1977), Experiments on Whistler wave filamentation and VLF Hiss in a laboratory plasma, *J. Phys. Colloques*, *38*(C6), C6–89–C6-102, doi:10.1051/jphyscol:1977609.

Taubenschuss, U., Y. V. Khotyaintsev, O. Santolík, A. Vaivads, C. M. Cully, O. Le Contel, and V. Angelopoulos (2014), Wave normal angles of whistler mode chorus rising and falling tones, *J. Geophys. Res. Space Physics*, *119*, 9567–9578, doi:10.1002/2014JA020575.

Thorne, R. M. (2010), Radiation belt dynamics: The importance of wave-particle interactions, *Geophys. Res. Lett.*, *37*, L22107, doi:10.1029/2010GL044990.

Thorne, R. M., B. Ni, X. Tao, R. B. Horne, and Meredith N. P. (2010), Scattering by chorus waves as the dominant cause of diffuse auroral precipitation, *Nature*, *467*, 943–946, doi:10.1038/nature09467.

Thorne, R. M., et al. (2013), Rapid local acceleration of relativistic radiation belt electrons by magnetospheric chorus, *Nature*, *504*, 411–414, doi:10.1038/nature12889.

Trakhtengerts, V. Y., A. G. Demekhov, E. E. Titova, B. V. Kozelov, O. Santolik, D. Gurnett, and M. Parrot (2004), Interpretation of Cluster data on chorus emissions using the backward wave oscillator model, *Phys. Plasmas*, *11*, 1345–1351, doi:10.1063/1.1667495.

Tsurutani, B. T., and E. J. Smith (1974), Postmidnight chorus: A substorm phenomenon, *J. Geophys. Res.*, *79*, 118–127, doi:10.1029/JA079i001p00118.

Verkhoglyadova, O. P., B. T. Tsurutani, and G. S. Lakhina (2010), Properties of obliquely propagating chorus, *J. Geophys. Res.*, *115*, A00F19, doi:10.1029/2009JA014809.

Wang, K., C.-H. Lin, L.-Y. Wang, T. Hada, Y. Nishimura, D. L. Turner, and V. Angelopoulos (2014), Pitch-angle distributions of electrons at dipolarization sites during geomagnetic activity: THEMIS observations, *J. Geophys. Res. Space Physics*, *119*, 9747–9760, doi:10.1002/2014JA020176.

Yagitani, S., T. Habagishi, and Y. Omura (2014), Geotail observation of upper band and lower band chorus elements in the outer magnetosphere, *J. Geophys. Res. Space Physics*, *119*, 4694–4705, doi:10.1002/2013JA019678.

Yamaguchi, K., T. Matsumoto, Y. Omura, and D. Nunn (2013), Ray tracing of whistler-mode chorus elements: Implications for generation mechanisms of rising and falling tone emissions, *Ann. Geophys.*, *31*, 665–673, doi:10.5194/angeo-31-665-2013.

Zhang, Y. L., H. Matsumoto, and Y. Omura (1993), Linear and nonlinear interactions of an electron beam with oblique whistler and electrostatic waves in the magnetosphere, *J. Geophys. Res.*, *98*(A12), 21,353–21,363, doi:10.1029/93JA01937.